Cement & Concrete Composites 35 (2013) 171–180

Contents lists available at SciVerse ScienceDirect

Cement & Concrete Composites

journal homepage: www.elsevier.com/locate/cemconcomp

Cement-modified enamel coating for enhanced corrosion resistance of steel reinforcing bars

Fujian Tang [a], Genda Chen [a,*], Jeffery S. Volz [a], Richard K. Brow [b], Michael L. Koenigstein [c]

[a] Department of Civil, Architectural, and Environmental Engineering, Missouri University of Science and Technology, Rolla, MO 65409-0030, USA
[b] Department of Materials Science and Engineering, Missouri University of Science and Technology, Rolla, MO 65401, USA
[c] Pro-Perma Engineered Coatings, Hypoint, Rolla, MO 65401, USA

ARTICLE INFO

Article history:
Received 28 June 2012
Received in revised form 16 August 2012
Accepted 16 August 2012
Available online 25 August 2012

Keywords:
Corrosion
Cement modified enamel
SEM
EIS
Chloride

ABSTRACT

The corrosion performance of smooth steel rebar coated with pure enamel, mixed enamel, and double enamel, and embedded in mortar cylinders were quantified in 3.5 wt.% NaCl solution using open-circuit potential (OCP), linear polarization resistance (LPR), and electrochemical impedance spectroscope (EIS) tests over a period of 173 days. The mixed enamel was prepared by adding calcium silicate contained in cement into the pure enamel. The double enamel consisted of an inner pure enamel layer and an outer mixed enamel layer. Results indicated that after 27 days of immersion, corrosion initiated and was rapidly developed in uncoated and the mixed enamel coated specimens. Although the OCP indicated a high likelihood of corrosion initiation, the pure enamel and double enamel coated rebar had significantly lower corrosion current densities, and thus remained in passivity throughout the entire test period. This behavior was further verified by the forensic study and EIS results.

1. Introduction

Steel rebar in concrete is generally protected by a thin passive film formed due to the high alkalinity of fresh concrete pore solution [1,2]. However, this thin film can be degraded by the penetration of carbon dioxide and aggressive ions such as chloride [3,4]. When this happens, corrosion will initiate in the presence of moisture and oxygen, resulting in the formation of corrosion products that are usually several times greater in volume than the original steel consumed. These expansive corrosion products may lead to cracking and spalling of concrete cover, which is a typical consequence of corrosion of steel in concrete. In addition, corrosion may impair structural capacity through reduction of reinforcement cross section and the loss of bond between reinforcement and concrete [5–8]. Corrosion protection of steel rebar is often achieved by adding inhibitors in concrete [9–11], using high performance concrete mixtures [12–14], using protective coatings [15–18], using stainless steel [19,20], and applying cathodic protection [21,22]. Among these methods, use of protective coatings is the most economical and effective method since it can establish a physical barrier between aggressive ions and the steel rebar.

Porcelain enamel is a vitreous or glassy inorganic coating bonded to the substrate metal by fusing glass frits at a temperature of 750–850 °C. It has been extensively used in domestic and industrial applications that require chemical, high temperature, corrosion and mechanical protection [23]. The properties of enamel coating are flexible and can be controlled by altering the chemical composition or microstructure, and pre-treating the metal substrate [24,25]. For example, replacing B_2O_3 with SiO_2/TiO_2 can increase the corrosion resistance of enamel in acidic environments; adding ZrO_2 can improve the performance of enamel in alkaline environments; increasing CoO and NiO can promote adherence of the enamel to a metal substrate; and crystallization treatment can improve the hardness of the coating [26]. Therefore, enamels can be designed and used to improve corrosion resistance in an alkaline environment with an enhanced chemical bond to the steel substrate [27], resulting in an alternative coating for steel rebar applied in concrete structures.

In a recent study by the authors [28], the microstructure and phase composition of three types of enamel coating (pure, mixed, and double enamels) have been examined using SEM and XRD techniques, and their corrosion resistances were characterized in 3.5 wt.% NaCl solution with open-circuit potential, electrochemical impedance spectroscope and potentiodynamic polarization methods. The test results showed that all three enamel coatings can improve the corrosion resistance of steel rebar to various extents. However, the effectiveness of these enamel coatings to protect steel rebar from corrosion in an application environment in

* Corresponding author. Address: Department of Civil, Architectural, and Environmental Engineering, Missouri University of Science and Technology, 328 Butler-Carlton Hall, 1401 N. Pine Street, Rolla, MO 65409-0030, USA.
E-mail address: gchen@mst.edu (G. Chen).

0958-9465/$ - see front matter © 2012 Elsevier Ltd. All rights reserved.
http://dx.doi.org/10.1016/j.cemconcomp.2012.08.009

concrete/mortar, and more importantly, the change in their corrosion resistance over time have not been well understood. In addition, a comprehensive evaluation of the corrosion process over time, including chloride ion ingress, passive film degradation, and corrosion resistance degradation of enamel coated rebar have never been studied systematically.

This study aims to investigate the time-varying corrosion performances of three types of enamel coating in 3.5 wt.% NaCl solution with enamel coated, smooth steel rebar embedded in ordinary Portland cement mortar cylinders. The chloride ion ingress, passive film degradation, and corrosion resistance degradation of enamel coatings were investigated over a period of 173 days, using chloride content, open-circuit potential (OCP), linear polarization resistance (LPR), and electrochemical impedance spectroscope (EIS) tests. After various tests, each mortar cylinder was removed and the exposed rebar surface was visually inspected and examined with an optical microscope for signs of corrosion.

2. Experimental procedures

2.1. Preparation of enamel coatings and mortar cylinders

Enamels are typically silicate-based oxides that are deposited from slurries and fused at high temperature. The enamel slurry is prepared by milling glass frits, clay and certain electrolytes, then mixing with water to provide a stable suspension. Three types of enamels were investigated in this study: pure enamel, mixed enamel, and double enamel. Pure enamel served as a benchmark coating commercially available. Mixed enamel is a mixture of pure enamel and calcium silicate. The mixed enamel was introduced to enhance the strength of bond between steel bars and their surrounding concrete by increasing its surface roughness for mechanical bond and promoting its chemical reaction with cement for chemical bond. The double enamel was introduced to combine the superior corrosion performance of pure enamel and the better bond behavior of mixed enamel. It consisted of an inner pure enamel layer and an outer mixed enamel layer to increase its corrosion resistance through the inner layer and enhance its bond strength through the outer layer.

The pure enamel slurry was made by first adding 454 kg alkali borosilicate glass frits to 189.3 L water and mixing them for 20 min, and then adding 31.8 kg clay and 2.3 kg borax as suspension agents, and mixing again for 3.5 h. The chemical composition of alkali borosilicate glass frit is given in Table 1 [29]. This glass frit was selected because it contains ZrO_2 to improve the resistance of enamels in alkaline environments, and NiO and CoO to enhance the adherence strength with steel rebar. The mixed enamel was prepared by mixing 50% calcium silicate directly taken from the Portland cement [30] with the 50% pure enamel. The mixed enamel slurry was made following the same procedure as the pure enamel slurry.

Commercial steel rebar (12.7 mm diameter) was used in this study, and its chemical composition was determined and is given in Table 2. Prior to enamel coating, all steel rebar was sand-blasted and cleansed with a commercially available cleansing solvent. For PE and ME coatings, the cleaned steel rebar was dipped into their corresponding liquid slurry, heated for 2 min at 150 °C to drive off moisture, fired at 810 °C for 10 min, and finally cooled to room temperature. For the DE coating, the steel rebar was first dipped into the PE slurry and heated for 2 min at 150 °C to drive off moisture, then dipped into the ME slurry and heated to 150 °C again to drive off moisture, finally fired for 10 min at 810 °C. The firing treatment at high temperature was used to melt the glass frit and chemically bond the enamel to the steel rebar.

Mortar was prepared using a mixture of cement, fine aggregate and water. Type I Portland cement was used, and its chemical composition is listed in Table 3. Missouri River sands were used as fine aggregates with a maximum size of 6.35 mm and a fineness modulus of 2.80. The water/cement ratio was 0.55. The proportion of sand used in the mix was 2.81 times the weight of the cement.

Cylindrical mortar specimens were prepared as shown in Fig. 1a; each cylinder is 38.1 mm in diameter and 114.3 mm tall. One 88.9 mm long steel rebar specimen, either uncoated or enamel coated, was placed along the centerline of the cylinder as shown in Fig. 1a. A copper wire was welded to the top end of the rebar to provide an electrical connection. To force the corrosion activity in the middle portion of the steel rebar and avoid any potential crevice corrosion at the two ends, each end of the rebar was encased in a PVC tube filled with epoxy resin. Therefore, the actual length of rebar potentially exposed to the corrosive environment was approximately 50.8 mm, with a surface area of approximately 20.3 cm^2. The clear cover of mortar around the exposed portion of the rebar was 12.7 mm. For the casting of each specimen, a PVC pipe with a nominal inside diameter of 38.1 mm was used as a mold, and the steel rebar and the PVC mold were held in place by grooves pre-cut on a bottom plywood sheet as shown in Fig. 1b and c. To ensure a proper consolidation, each mortar specimen was cast in three layers, each compacted 25 times with a 6.35-mm-diameter steel rod and tapped 15 times with a small rubber mallet on the PVC mold to close the potential void generated by each rodding/compaction. All specimens were de-molded after 24 h, placed in a curing room at room temperature and 100% relative humidity, and cured for 28 days prior to testing. Three identical specimens were prepared for each condition, and the specimen whose test result lies in between the other two was selected to represent the coating system. For reference, mortars with uncoated steel rebar were also prepared at the same time.

2.2. Mortar/steel interface

The microstructure of the interfaces between the mortar and steel rebar was investigated through scanning electron microscope (SEM, Hitachi S4700). One 8.0 mm thick cross section of mortar was sectioned with a diamond blade for each of the uncoated, PE, ME, and DE coated steel rebar reinforced specimens. The slices were polished using silicate carbide papers with grits of 80, 180, 320, 600, 800 and 1200, rinsed with de-ionized water, and placed in an oven prior to the SEM study. Mounting epoxy was cast around each specimen to protect the mortar and enamel coating from damage during the sample preparation.

2.3. Chloride measurement

Six additional mortar cylinders without steel rebar were prepared to monitor the diffusion process of chloride ions over time. One cylinder was removed from the NaCl solution approximately every 30 days and sectioned with a diamond blade into two halves with one cross section schematically illustrated in Fig. 2. Mortar

Table 1
Chemical composition of alkali borosilicate glass frit.

Materials	SiO_2	B_2O_3	Na_2O	K_2O	CaO	CaF_2	Al_2O_3	ZrO_2	CoO	MnO_2	NiO
Wt.%	44.0	19.3	15.8	2.8	0.0	4.7	4.6	5.3	0.9	1.5	1.0

Table 2
Chemical composition of steel rebar.

Element	C	Si	Mn	P	S	Cr	Mo	Ni	Co	Cu	V	Sn	Fe
Wt.%	0.43	0.22	0.95	0.15	0.07	0.17	0.03	0.10	0.01	0.46	0.02	0.02	97.37

Table 3
Chemical composition of Type-I Portland cement (wt.%).

Loss on ignition	SiO_2	Al_2O_3	CaO	MgO	SO_3	Na_2O	K_2O	Cl	TiO_2	Fe_2O_3	P_2O_5	Total
3.98	19.48	6.80	55.35	3.32	4.35	2.39	1.00	0.02	0.20	2.18	0.19	99.27

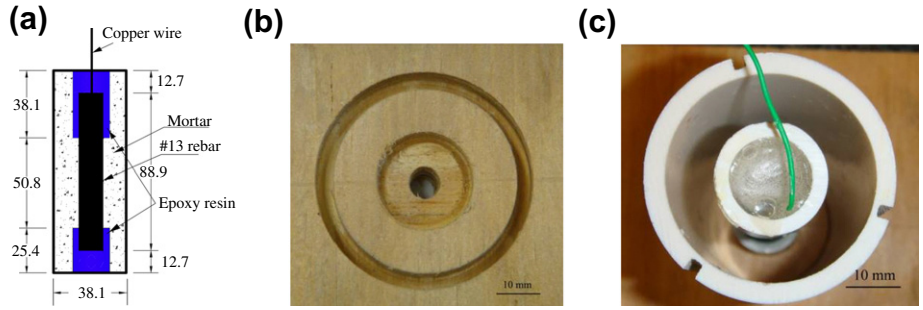

Fig. 1. Mortar cylinder specimens: (a) geometries (unit: mm), (b) groove precut on plywood, and (c) PVC mold for casting.

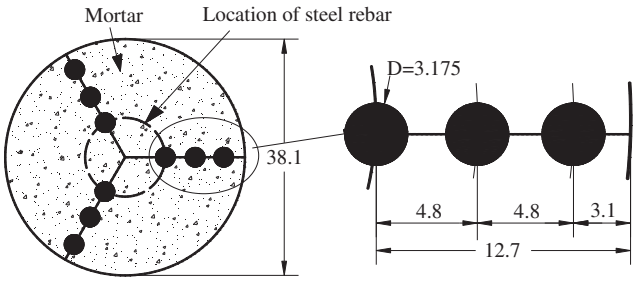

Fig. 2. Locations of mortar powder samples for chloride content analysis (unit: mm).

powder samples were taken directly from the middle cross section to avoid disproportionately high chloride contents at the top and bottom of the specimen. The samples were collected using a 3.175-mm-diameter masonry drill bit at each of three depths from the cylinder side face: 3.1 mm, 7.9 mm, and 12.7 mm, as indicated in Fig. 2. To collect representative data points, powder samples were taken from three locations evenly distributed around the circumference of the cylinder. The three samples at each respective depth were mixed together for chloride analysis, totaling 1.5 g. Using Rapid Chloride Testing equipment manufactured by German Instruments, Inc., the concentration of water soluble chlorides contained within each powder sample was determined.

2.4. Electrochemical measurements

All mortar cylinders were immersed up to 173 days in glass beakers that contained 3.5 wt.% NaCl solution at room temperature and open to the air. The solution was made by mixing the purified sodium chloride with distilled water. To maintain a constant concentration of the test solution, distilled water was added every 2 days to compensate for any evaporative loss. OCP, LPR and EIS measurements were performed approximately every 30 days, and prior to testing, the NaCl solution was replaced with fresh solution to avoid any contamination of the electrolyte. All electrochemical measurements used a three-electrode test setup consisting of a 25.4 mm × 25.4 mm × 0.254 mm platinum sheet as a counter electrode, a saturated calomel electrode (SCE) as a reference electrode, and the mortar cylinder and rebar as a working electrode. These electrodes were connected to a Gamry, Reference 600 potentiostat/galvanostat/ZRA for data acquisition. EIS measurements were taken at five points per decade with a sinusoidal potential of 10 mV applied around the open-circuit potential E_{ocp} with a frequency range of 5 mHz–100 kHz. The LPR curves were measured within $E_{ocp} \pm 15$ mV at a scan rate of 0.167 mV/s. Representing the slope of the polarization curve, the polarization resistance, R_p, can be calculated by:

$$R_p = \Delta V/\Delta i \tag{1}$$

where ΔV and Δi represent the voltage and current increments, respectively, in the linear portion of the polarization curve at $i = 0$. LPR measurements were used to calculate the corrosion current density by the Stern-Geary equation [31]:

$$i_{corr} = \beta_a\beta_c/[2.303(\beta_a + \beta_c)R_p] = B/R_p \tag{2}$$

where i_{corr} is the corrosion current density, β_a is the anodic Tafel slope, β_c is the cathodic Tafel slope, and B is a constant related to β_a and β_c. In this study, a tentative value of 26 mV for the B constant was used [32,3].

2.5. Visual observation

After 173 days of immersion testing, all mortar cylinders were removed from the NaCl solution and dried in an oven at 60 °C for 1 day. The dry mortar cylinders were removed from the steel rebar using a steel hammer, and the surface condition of the exposed steel rebar was examined with an optical microscope.

3. Results and discussion

3.1. Mortar/steel interfaces

Fig. 3 shows SEM images of the interfaces between the mortar and coated/uncoated steel rebar prior to immersion test. For uncoated steel rebar, a passive film was formed due to the high alkaline mortar pore solution. This passive film is very thin, less than 10 nm as observed with XPS techniques by other researchers [33,34]. Therefore, it cannot be identified with the relatively low magnification in Fig. 3a. Fig. 3b shows that the pure enamel coating has bubbles that were released from the reaction of the enamel coating with the steel during the enameling process. These bubbles are isolated and smaller than the coating thickness (150 μm). As shown in Fig. 3c, the mixed enamel coating, 300 μm thick, has a porous structure with interconnected channels that were generated due to an increase in the viscosity of the mixed enamel slurry as it was heated during firing. The double enamel coating, 250 μm thick, has similar microstructure to the pure enamel coating as indicated in Fig. 3d.

3.2. Open-circuit potential, corrosion rate and chloride profile

Fig. 4 is a plot of the OCP as a function of time up to 173 days for mortar samples with uncoated and enamel coated steel rebar immersed in 3.5 wt.% NaCl solution. The OCP values of all cylinders were larger than −273 mV/SCE at the beginning of testing and dropped below −273 mV/SCE at 27 days. According to ASTM C876 [35], the probability of the initiation of corrosion is 90% at 27 days. The OCP values then remained approximately −700 mV/SCE and −520 mV/SCE for mortar specimens with uncoated and enamel coated steel reinforcement, respectively. Initiation of corrosion for mortar cylinders with uncoated steel rebar is due to breakdown of the passive film induced by chloride ions. For cylinders with mixed enamel coated steel rebar, the penetration of chlorides through connected channels inside the coating initiated corrosion. For pure enamel and double enamel coated samples, the initial decrease in OCP may indicate the onset of corrosion due to small defects that are inherent in the enamel coating process.

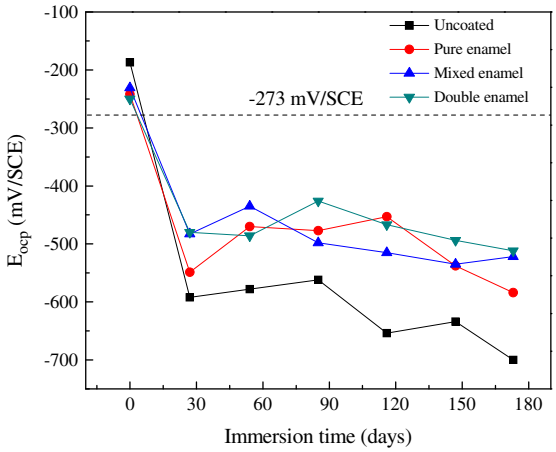

Fig. 4. Open-circuit potential evolution with time for mortar cylinders reinforced with uncoated and three types of enamel coated steel rebar in 3.5 wt.% NaCl solution.

Fig. 5 shows the change of corrosion current density as a function of time by the LPR tests. According to the Durar Network Specification [32], the corrosion level may be divided into four levels: passivity when $i_{corr} < 0.1$ μA/cm^2, low corrosion when 0.1 μA/cm^2 < i_{corr} < 0.5 μA/cm^2, high corrosion when 0.5 μA/cm^2 < i_{corr} < 1.0 μA/cm^2, and very high corrosion when 1.0 μA/cm^2 < i_{corr}. Cylinders with uncoated steel rebar experienced all four states: passive state at the beginning of immersion, low corrosion after 27 days, high corrosion from 54 days to 85 days, and very high corrosion after 116 days. Cylinders with the mixed enamel coated steel rebar had similar behaviors but reached a high corrosion level after 116 days of immersion, which indicated a greater corrosion resistance than the uncoated steel rebar. Mortar cylinders with the pure enamel and double enamel coated steel rebar remained in the passive state throughout the test. The corrosion current density ranged from 0.019 to 0.039 μA/cm^2 for mortar cylinders with the pure enamel coated rebar and from 0.003 to 0.004 μA/cm^2 for mortar cylinders with the double enamel coated rebar. The fact that the double enamel coated samples have a lower corrosion

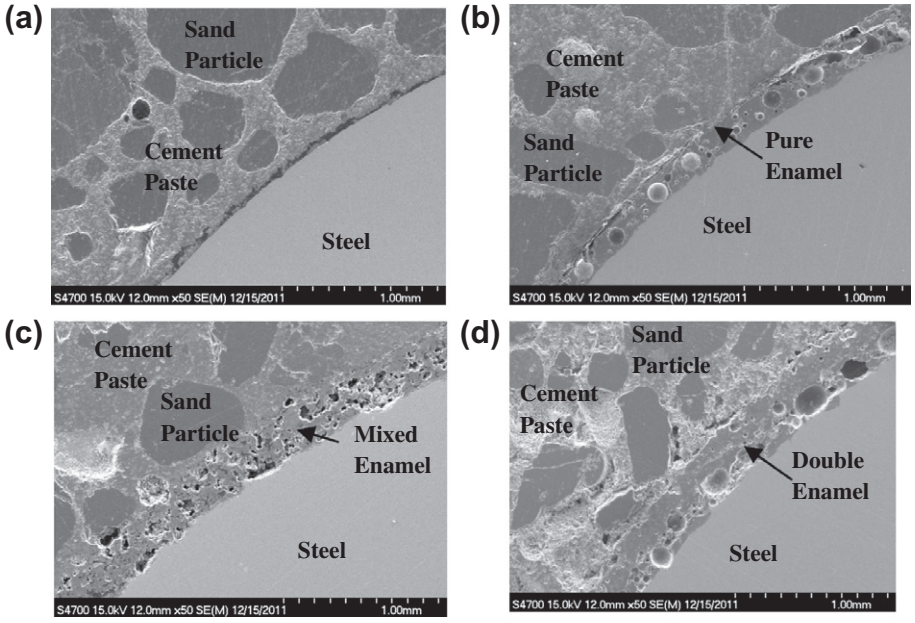

Fig. 3. Cross sectional SEM images of the interface between mortar and steel rebar for: (a) uncoated, (2) pure enamel coated, (c) mixed enamel coated, and (d) double enamel coated.

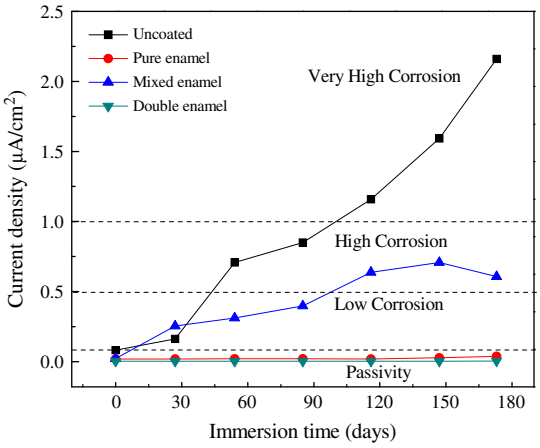

Fig. 5. Corrosion current density evolution with time for mortar cylinders reinforced with uncoated and three types of enamel coated steel rebar in 3.5 wt.% NaCl solution.

current density than the pure enamel coated rebar is mainly attributed to the thicker double enamel coating as illustrated in Fig. 3b and d. Note that the corrosion current density from LPR tests seems inconsistent with the OPC results at a first glimpse. This is because the areas of the defects in the pure enamel and double enamel coatings are very small, resulting in an overall small corrosion current density defined over the entire coating area exposed to the corrosive solution. For the mixed enamel coating, the defects formed during the high temperature firing are interconnected and covered a more significant area. As a result, the corrosion current for the mixed enamel coating is substantially higher than those of the pure and double enamel coatings as indicated in Fig. 5.

Corrosion of steel rebar initiates when the chloride content on the rebar surface exceeds the chloride threshold, which is a function of mortar mix, exposure condition, cement type, and so on. ACI Building Code 318 [36] specifies the maximum water-soluble chloride content in concrete in a chloride rich environment to be 0.15% by weight of cement. According to Mehta [37], the level of chloride content that causes the breakdown of passive film on the surface of steel ranges from 0.23% to 1.5%. Fig. 6 shows the change in chloride distribution over time for mortar cylinders in 3.5 wt.% NaCl solution. It can be observed from Fig. 6 that the chloride content at the location of the steel rebar surface (11 mm from the mortar surface) in similar mortar cylinders with steel rebar was 0.25% after the mortar cylinders had been immersed in the

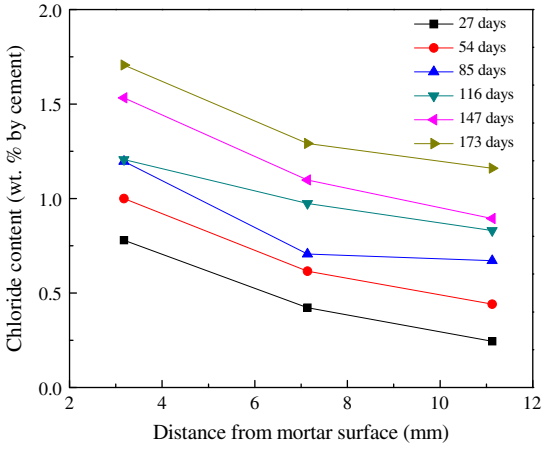

Fig. 6. Chloride distribution in mortar with time in 3.5 wt.% NaCl solution.

NaCl solution for 27 days, and increased to 1.25% after 173 days. Therefore, the mortar cylinders had accumulated sufficient chloride ions for breakdown of the passive film and the initiation of corrosion when the initial tests were made.

3.3. EIS results

Fig. 7 shows the impedance diagrams of mortar cylinders with uncoated and three types of enamel coated steel rebar up to 173 days. The phase-frequency plots in Fig. 7a-3 and c-3 indicated three time constants for cylinders with the uncoated and mixed enamel coated steel rebar, regardless of immersion time. The first time constant in the high frequency range (>10^4 Hz) is associated with the dielectric properties of the mortar or combined mortar and mixed enamel coating [38]. The second time constant in the middle frequency range (1–10^4 Hz) is likely attributed to the dielectric properties of the passive layer formed on the steel rebar surface due to the high alkalinity of the fresh mortar pore solution during cement hydration process. The presence of the passive layer for cylinders with the mixed enamel coated steel rebar is due to the penetration of mortar pore solution through the connected channels to the steel surface. The third time constant in the low frequency range (<1 Hz) is closely related to the interface properties between steel rebar and mortar or enamel coating where corrosion occurs, namely the double layer capacitance and charge transfer resistance. The change of impedance spectra over time can only be reflected by the third time constant in the low frequency range.

Mortar cylinders with the pure enamel and double enamel coated steel rebar had different behaviors from those with the uncoated and mixed enamel coated reinforcement. Regardless of the immersion time, these specimens can be represented by two time constants as indicated in Fig. 7b-3 and d-3. The impedance magnitudes of these two types of mortar cylinders, Fig. 7b-2 and d-2, were higher than those with the uncoated and mixed enamel coated steel rebar at all frequencies, Fig. 7a-2 and c-2. The time constant in the high frequency range (>10^3 Hz for pure enamel and >10^2 Hz for double enamel) is associated with the dielectric properties of combined mortar and enamel coating. The second time constant in the low frequency range (<10^3 Hz for pure enamel and <10^2 Hz for double enamel) originated from the interface properties due to the charge transfer resistance and double layer capacitance.

The intrinsic dielectric properties of mortar/enamel coating and passive film as well as the electrochemical behavior at the mortar–steel interface can be obtained by fitting an appropriate equivalent electrical circuit (EEC) model to the EIS test data. As illustrated in Fig. 8, two EEC models were used in this study: (a) with two distributed constant phase elements (CPEs) for mortar cylinders with the pure enamel and double enamel coated steel rebar and (b) with three distributed CPEs for mortar cylinders with the uncoated and mixed enamel coated steel rebar. Model (a) consists of a salt solution resistance R_s, capacitance CPE_m and resistance R_m of bulk-matrix (combined mortar and enamel coating for pure enamel and double enamel), charge transfer resistance R_{ct}, and double layer capacitance CPE_{dl}. Such a model was used by other researchers to study steel corrosion in carbonated alkali-activated slag concrete [29]. Model (b) consists of a solution resistance R_s, bulk-matrix (mortar or mortar and mixed enamel coating) capacitance CPE_m and resistance R_m, passive film capacitance CPE_f and resistance R_f, charge transfer resistance R_{ct}, and double layer capacitance CPE_{dl}. A model similar to (b) was used to study the electrochemical characteristics of reinforced concrete corrosion [39].

Application of CPEs in the EEC models is attributed to the non-homogeneity of the system under study. The non-homogeneity mainly comes from the irregularities on the steel surface, surface roughness, fractal surface, and in general certain processes

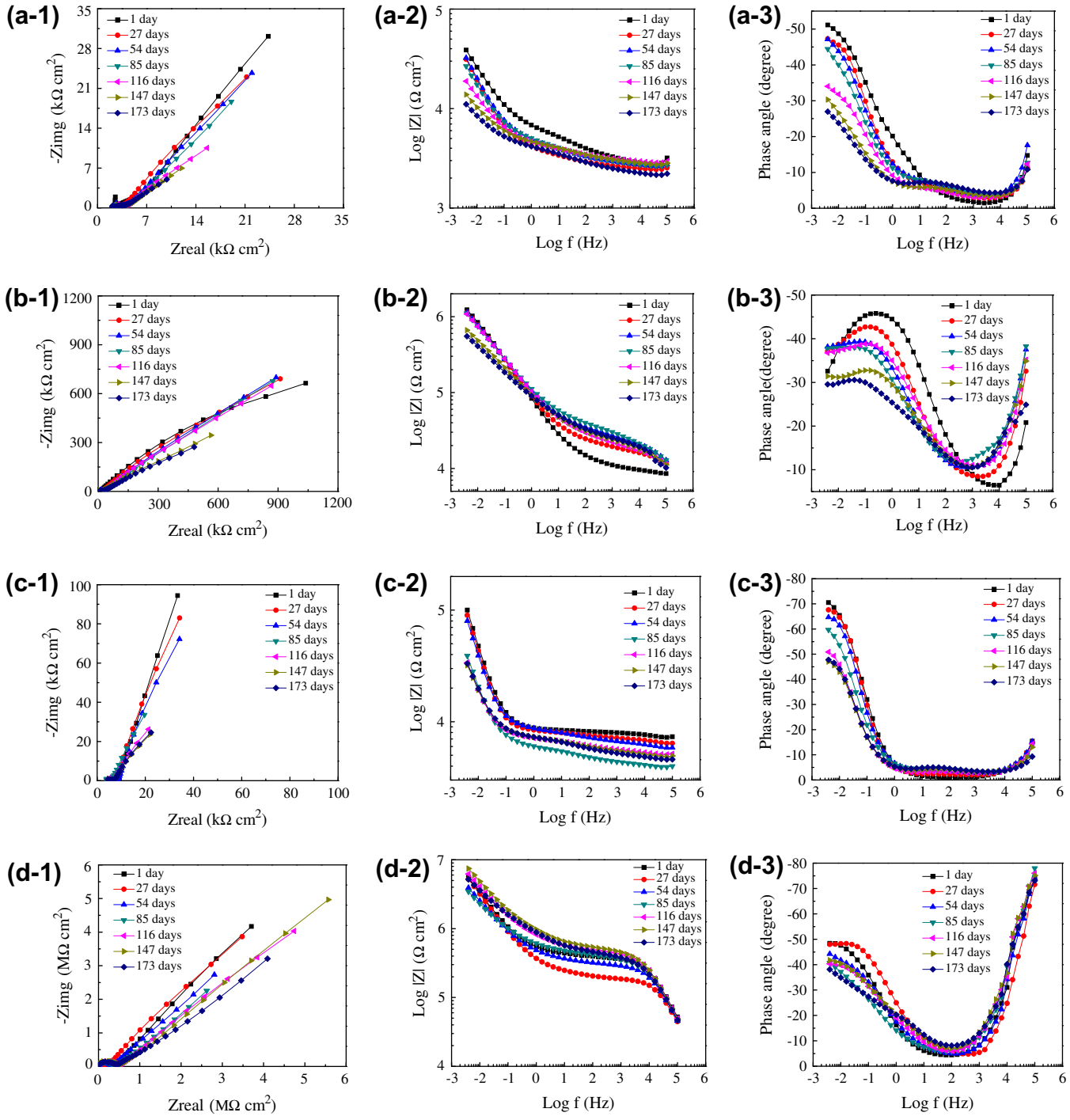

Fig. 7. Typical EIS diagrams of mortar cylinders in 3.5 wt.% NaCl solution with: (a) uncoated, (b) pure enamel, (c) mixed enamel, and (d) double enamel coated steel rebar in the format of Nyquist plots(1), and Bode plots (2) and (3).

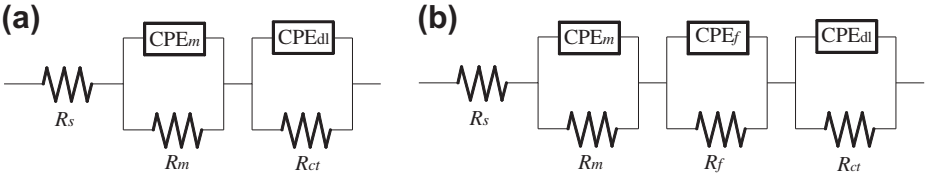

Fig. 8. Equivalent electrical circuits for mortar cylinders with: (a) pure enamel and double enamel coated steel rebar and (b) uncoated and mixed enamel coated steel rebar.

associated with an irregular distribution of the applied potential [19]. The CPE is defined by two parameters Y and n, and its admittance representation is:

$$Y_{CPE} = Y(j\omega)^n \quad (3)$$

where Y is a parameter with dimension of Ω^{-1} cm^{-2} s^n, which is directly proportional to the capacitance of pure capacitive electrode [40], ω is the angular frequency in rad/s, and n represents the deviated degree of the capacitance of the electrode from the ideal condition of a pure capacitor. When $n = 1$, the CPE resembles a capacitor with capacitance Y; when $n = 0.5$, it represents Warburg impedance; when $n = 0$, the CPE represents a resistor with resistance Y^{-1}, and when $n = -1$, it is an inductor.

ZsimpWin software [41] was used to fit all EIS data. The Chi-squared value was found to be on the order of 10^{-3} for all results, indicating a good simulation with the proposed two EEC models. For example, Fig. 9 shows the excellent agreement between the EEC models and the results of four types of mortar cylinders after 116 days of immersion.

Tables 4 and 5 summarize the EEC model parameters for mortar cylinders with the uncoated and three types of enamel coated steel rebar. The solution resistance R_s was close to zero when the dielectric properties of the bulk-matrix were extracted by extending the small arc in the high frequency range to the real axis. It was therefore not listed in the tables.

The bulk-matrix resistance and capacitance reflect the ability of the mortar/enamel coating to resist the penetration of electrolytes containing aggressive ions and the dielectric properties of the mortar/enamel coating, respectively, both closely related to the porosity of mortar and enamel coatings. As shown in Table 4, for mortar cylinders with the uncoated steel rebar, the bulk-matrix (mortar) resistance is in the range of 2.68–3.41 kΩ cm^2. For cylinders with the mixed enamel coated steel rebar, the mortar and mixed enamel coating resistance is in the range of 3.96–6.91 kΩ cm^2, which is approximately twice as high as that for the uncoated steel rebar. This is likely because the mixed enamel coating has a higher resistivity than the mortar, despite the presence of connected channels. Capacitance Y_m of the bulk-matrix is in the range of 0.10–4.06 nΩ^{-1} cm^{-2} s_m^n for the uncoated and 0.47–13.2 nΩ^{-1} cm^{-2} s_m^n for the mixed enamel coated specimen, respectively. This range is in reasonable agreement with other studies in the literature [32,39].

As shown in Table 5, the bulk-matrix resistance of mortar cylinders with the pure enamel coated rebar is in the range of 8.21–26.9 kΩ cm^2, which is higher than that for the uncoated and mixed enamel coated rebar. This is attributed to the improved barrier behavior of the pure enamel coating, despite the isolated pores in the coating. The bulk resistance of the double enamel coating is in the range of 193–483 kΩ cm^2, which is approximately 100 times higher than that with the uncoated steel bar. This is because the double enamel coating has a relatively thicker coating than the pure enamel coating. The capacitance of the bulk-matrix is in the range of 0.67–0.92 nΩ^{-1} cm^{-2} s_m^n for the pure enamel coated and 0.83–0.86 nΩ^{-1} cm^{-2} s_m^n for the double enamel coated, respectively. These values are smaller than the uncoated and mixed enamel coated, indicating substantial protection from the penetration of electrolytes through the pure and double enamel coatings.

For the uncoated and mixed enamel coated steel rebar, the resistance of the passive films varies between 1.0 and 3.2 kΩ cm^2, and the capacitance is in the range of 10–60 μΩ^{-1} cm^{-2} s_f^n. No change in passive film dielectric property was observed for the uncoated steel rebar even when the passive film was broken down by chloride attack. This is likely because the dielectric property of the passive film is close to that of the corrosion products.

The two most direct parameters to reflect corrosion resistance are charge transfer resistance and double layer capacitance. These parameters are related to the charge transfer during the corrosion process at the interface between the exposed steel and the electrolyte inside mortar pore structure; they are a measure of ease of corrosion [42]. For specimens with the uncoated steel rebar, the charge transfer resistance displayed a continuous reduction with time of immersion from 285 to 36 kΩ cm^2, indicating a transition from the passive state to the active state. The same trend was also observed

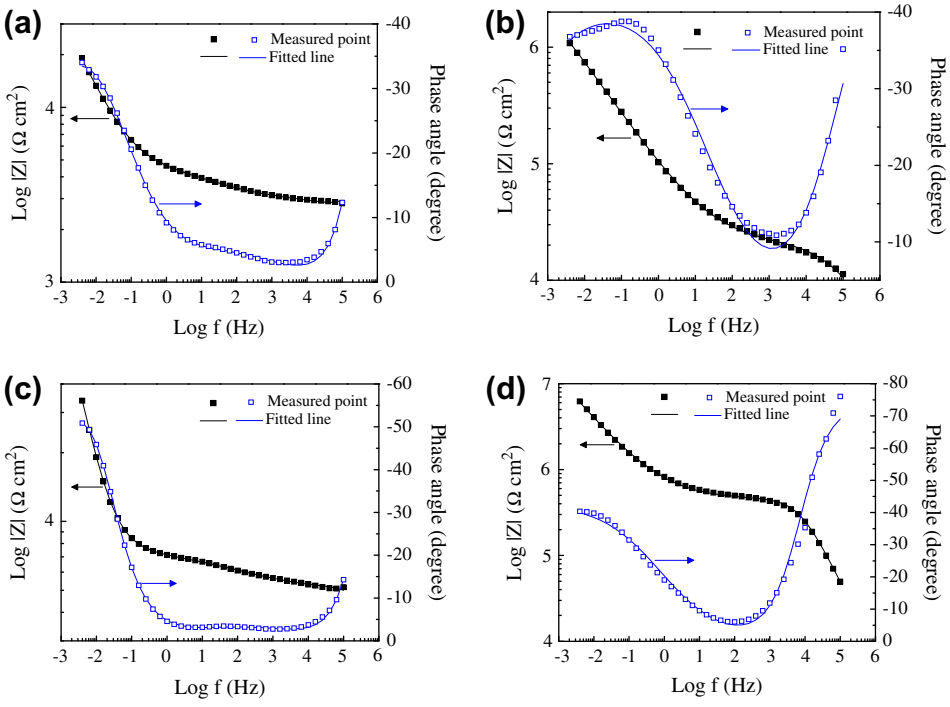

Fig. 9. Measured versus simulated impedance spectra for: (a) uncoated, (2) pure enamel, (c) mixed enamel, and (d) double enamel coated steel rebar after 116 days of immersion in 3.5 wt.% NaCl solution.

Table 4
EEC model (b) parameters for mortar cylinders with uncoated and mixed enamel coated steel rebar in 3.5 wt.% NaCl solution.

Time (day)	R_m (kΩ cm^2)	n_m	Y_m (nΩ^{-1} cm$^{-2}s_m^{-n}$)	R_f (kΩ cm^2)	n_f	Y_f (μΩ^{-1} cm$^{-2}s_f^n$)	R_{ct} (kΩ cm^2)	n_{dl}	Y_{dl} (μΩ^{-1} cm$^{-2}s_{dl}^n$)
Uncoated steel rebar									
0	2.79	0.80	1.03	1.04	0.44	16.8	285	0.70	164
27	2.68	1.00	0.11	4.71	0.20	28.2	188	0.71	629
54	3.05	1.00	0.10	3.07	0.26	11.5	198	0.62	652
85	2.95	0.96	0.21	3.13	0.29	92.2	102	0.59	770
116	3.41	0.55	4.06	1.15	0.47	54.3	76	0.48	502
147	3.39	0.77	2.07	1.81	0.41	48.6	43	0.49	757
173	3.18	0.87	0.46	2.25	0.38	52.7	36	0.52	795
Mixed enamel coated steel rebar									
0	6.41	0.87	0.47	2.36	0.19	42.5	960	0.84	226
27	6.91	0.72	3.25	1.46	0.47	42.9	829	0.87	274
54	6.11	0.74	2.57	3.22	0.35	58.5	677	0.86	299
85	3.96	0.80	1.48	2.41	0.38	62.1	634	0.79	308
116	5.23	0.76	2.07	2.05	0.41	45.9	193	0.78	559
147	5.15	0.64	9.98	2.20	0.47	34.1	148	0.76	530
173	4.87	0.60	13.2	2.60	0.46	34.9	143	0.77	536

Table 5
EEC model (a) parameters for mortar cylinders with pure enamel and double enamel coated steel rebar in 3.5 wt.% NaCl solution.

Time (day)	R_m (kΩ cm^2)	n_m	Y_c (nΩ^{-1} cm$^{-2}s_m^n$)	R_{ct} (kΩ cm^2)	n_{dl}	Y_{dl} (μΩ^{-1} cm$^{-2}s_{dl}^n$)
Pure enamel coated steel rebar						
0	8.21	0.84	0.57	2410	0.54	4.12
27	14.2	0.71	3.78	3790	0.46	4.80
54	12.9	0.92	0.33	1910	0.58	8.54
85	20.5	0.81	1.22	3750	0.52	8.69
116	26.9	0.78	1.74	3460	0.43	7.07
147	21.4	0.67	7.85	3810	0.32	6.43
173	21.3	0.73	3.39	3350	0.48	11.9
Double enamel coated steel rebar						
0	387	0.85	0.23	>10^4	0.58	1.64
27	193	0.86	0.22	>10^4	0.57	1.62
54	303	0.85	0.26	>10^4	0.51	1.78
85	388	0.83	0.33	>10^4	0.46	1.75
116	455	0.84	0.27	>10^4	0.48	1.01
147	483	0.83	0.32	>10^4	0.47	0.81
173	381	0.83	0.34	>10^4	0.40	0.92

for the mixed enamel coated steel rebar from 960 to 143 kΩ cm^2. The charge transfer resistance of the double enamel coating exceeded 10^4 kΩ cm^2 and cannot be accurately obtained from the simulation since the obvious diffusion behavior appeared in the low frequency range. The charge transfer resistance of the pure enamel coated rebar is also large, ranging from 1910 to 3810 kΩ cm^2. Like the double enamel coating, the pure enamel coated rebar appeared to remain in a passive state over the entire duration of testing. These results were in agreement with the LPR results.

The double layer capacitance increased from 164 to 795 μΩ^{-1} cm^{-2} s_{dl}^n for mortar cylinders with the uncoated steel rebar and from 226 to 536 μΩ^{-1} cm^{-2} s_{dl}^n for mortar cylinders with the mixed enamel coated steel rebar, respectively. These results indicate that the diffusion of chloride ions increased the activity of corrosion at the double layer interface. The double layer capacitance ranged from 4.12 to 11.9 μΩ^{-1} cm^{-2} s_{dl}^n for mortar cylinders with the pure enamel coated steel rebar and from 0.81 to 1.78 μΩ^{-1} cm^{-2} s_{dl}^n for mortar cylinders with the double enamel coated steel rebar. The smaller double layer capacitance of the pure and double enamel coatings also indicated a higher corrosion resistance than the uncoated and mixed enamel coating.

3.4. Visual observation

Fig. 10 shows the surface condition of the uncoated and three types of enamel coated steel rebar after they were removed from mortar cylinders at the end of the 173 days of corrosion testing. As shown in Fig. 10, rust stains are apparent on the uncoated and the mixed enamel coated steel rebar only. No rust was observed on the pure enamel and double enamel coated steel rebar as shown in Fig. 10b and d. This observation verified the superior corrosion resistant performance of the pure and double enamel coatings as indicated by the LPR and EIS test results.

4. Conclusions

Based on the test data and analysis of 38.1-mm diameter mortar cylinders with embedded #13 smooth steel rebar, both uncoated and coated with three types of enamel, the following conclusions can be drawn:

1. Corrosion of the uncoated and mixed enamel coated steel rebar embedded in mortar cylinders initiated within 27 days of immersion in 3.5 wt.% NaCl solution, as supported by both the OCP and LPR tests. Based on the chloride analysis in mortar, the level of chloride content at the mortar–steel interface also indicated that the passive film on the steel rebar was most likely broken down and corrosion initiated after 27 days of immersion in the solution. The OCP of the tested specimens significantly decreased from above to below −273 mV/SCE and their corrosion current density increased from below the passivity threshold to a very high corrosion level and high corrosion level for uncoated and mixed enamel coated steel rebar at 173 days, respectively.

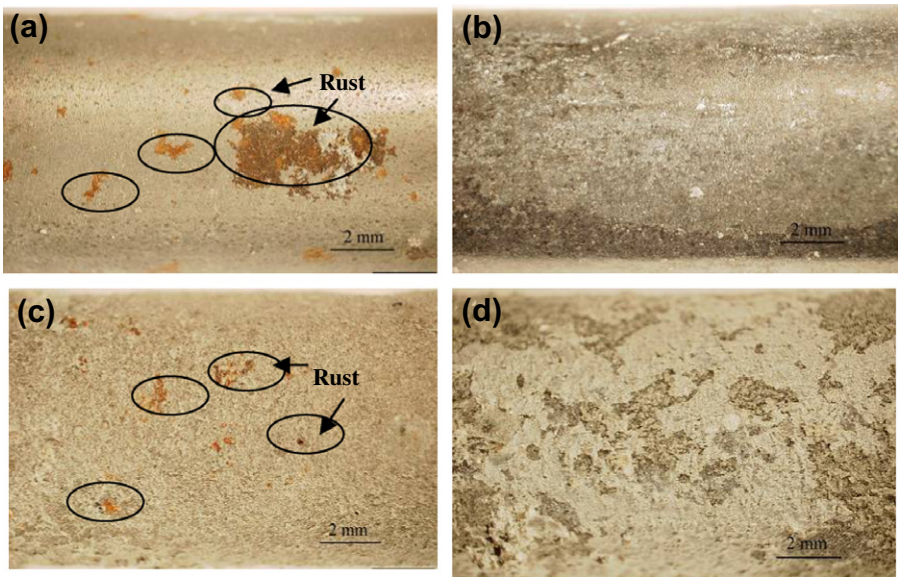

Fig. 10. Surface conditions of (a) uncoated, (b) pure enamel, (c) mixed enamel, and (d) double enamel coated steel rebar embedded in mortar after 173 days of immersion in 3.5 wt.% NaCl solution.

2. There was no sign of corrosion in pure enamel and double enamel coated steel rebar embedded in mortar cylinders. This finding was confirmed by visual inspections on the tested specimens at the end of corrosion testing. Although the OCP indicated a high probability of corrosion, the corrosion current density remained below the passivity threshold until the end of corrosion testing at 173 days.
3. The corrosion behavior of either uncoated or enamel coated rebar in mortar can be characterized by a single model throughout the corrosion tests. EIS tests indicated three time constants for mortar cylinders with uncoated and mixed enamel coated steel rebar, and two time constants for mortar cylinders with pure enamel and double enamel coated steel rebar. The first and last time constants correspond to the high and low frequency behaviors of the capacitive responses of mortar/enamel coating and the double layer interface, respectively. The middle time constant for uncoated and mixed enamel coated rebar in the middle frequency range is attributed to the dielectric property of the passive film since the mixed enamel coating has interconnected pore channels, extensively exposing steel rebar to the NaCl solution.

Acknowledgements

The authors gratefully acknowledge the financial support provided by National Science Foundation under Award No. CMMI-0900159. The findings and opinions expressed in this paper are those of the authors and do not necessarily reflect those of the sponsor.

References

[1] Ghods P, Isgor OB, McRae G, Miller T. The effect of concrete pore solution composition on the quality of passive oxide films on black steel reinforcement. Cem Concr Compos 2009;31(1):2–11.
[2] Feng X, Zuo Y, Tang Y, Zhao X, Lu X. The degradation of passive film on carbon steel in concrete pore solution under compressive and tensile stresses. Electrochim Acta 2011;58:258–63.
[3] Yu H, Chiang KTK, Yang L. Threshold chloride level and characteristics of reinforcement corrosion initiation in simulated concrete pore solutions. Constr Build Mater 2012;26(1):723–9.
[4] Bohni H. Corrosion in reinforced concrete structures. Cambridge, UK: Woodhead Publishing; 2005.
[5] Zhang R, Castel A, Francois R. Concrete cover cracking with reinforcement corrosion of RC beam during chloride-induced corrosion process. Cem Concr Res 2010;40(3):415–25.
[6] Shannag MJ, Al-Ateek SA. Flexural behavior of strengthened concrete beams with corroding reinforcement. Construct Build Mater 2006;20(9):834–40.
[7] Yi W, Kunnath SK, Sun X, Shi C, Tang F. Fatigue behavior of reinforced concrete beams with corroded steel reinforcement. ACI Struct J 2010;107(5):526–33.
[8] Xia J, Jin W, Li L. Shear performance of reinforced concrete beams with corroded stirrups in chloride environment. Corros Sci 2011;53(5):1794–805.
[9] Al-Amoudi OSB, Maslehuddin M, Lashari AN, Almusallam AA. Effectiveness of corrosion inhibitors in contaminated concrete. Cem Concr Compos 2003;25(4–5):439–49.
[10] Dhouibi L, Triki E, Raharinaivo A. The application of electrochemical impedance spectroscopy to determine the long-term effectiveness of corrosion inhibitors for steel in concrete. Cem Concr Compos 2002;24(1):35–43.
[11] Ormellese M, Berra M, Bolzoni F, Pastore T. Corrosion inhibitors for chlorides induced corrosion in reinforced concrete structures. Cem Concr Res 2006;36(3):536–47.
[12] Sun W, Zhang Y, Liu S, Zhang Y. The influence of mineral admixtures on resistance to corrosion of steel bars in green high-performance concrete. Cem Concr Res 2004;34(10):1781–5.
[13] Kayali O, Zhu B. Corrosion performance of medium-strength and silica fume high-strength reinforced concrete in a chloride solution. Cem Concr Compos 2005;27(1):117–24.
[14] Shi C. Corrosion resistance of alkali-activated slag cement. Adv Cem Res 2003;15(2):77–81.
[15] Bellezze T, Malavolta M, Quaranta A, Ruffini N, Roventi G. Corrosion behavior in concrete of three differently galvanized steel bars. Cem Concr Compos 2006;28(3):246–55.
[16] Almusallam AA, Khan FM, Dulaijan SU, Al-Amoudi OSB. Effectiveness of surface coatings in improving concrete durability. Cem Concr Compos 2003;25(4–5):473–81.
[17] Darwin AB, Scantlebury JD. Retarding of corrosion processes on reinforcement bar in concrete with an FBE coating. Cem Concr Compos 2002;24(1):73–8.
[18] Arenas MA, Casado C, Nobel-Pujol V, Damborenea J. Influence of the conversion coating on the corrosion of galvanized reinforcing steel. Cem Concr Compos 2006;28(3):267–75.
[19] Criado M, Bastidas DM, Fajardo S, Fernandez-Jimenez A, Bastidas JM. Corrosion behavior of a new low-nickel stainless steel embedded in activated fly ash mortars. Cem Concr Compos 2011;33(6):644–52.
[20] Garcia-Alonso MC, Escudero ML, Miranda JM, Vega MI, Capilla F, Correia MJ, et al. Corrosion behavior of new stainless steels reinforcing bars embedded in concrete. Cem Concr Res 2007;37(10):1463–71.
[21] Chess PM. Cathodic protection of steel in concrete. New York: Taylor & Francis; 1998.
[22] Hassanein AM, Glass GK, Buenfeld NR. Protection current distribution in reinforced concrete cathodic protection systems. Cem Concr Compos 2002;24(1):159–67.
[23] May 2012. <http://www.porcelainenamel.com/props.htm>.
[24] Jones DA. Principles and prevention of corrosion. New Jersey: Prentice Hall; 1996.

[25] Barcova K, Mashlan M, Zboril R, Filip J, Podjuklova J, Hrabovska K, et al. Phase composition of steel-enamel interfaces: effects of chemical pre-treatment. Surf Coat Technol 2006;201(3–4):1836–44.
[26] Wang D. Effect of crystallization on the property of hard enamel coatings on steel substrate. Appl Surf Sci 2009;255(8):4640–5.
[27] Yan D, Reis S, Tao X, Chen G, Brow RK, Koenigstein M. Effect of chemically reactive enamel coating on bonding strength at steel/mortar interface. Construct Build Mater 2012;28(1):512–8.
[28] Tang F, Chen G, Volz JS, Brow RK, Koenigstein M. Microstructure and corrosion resistance of enamel coatings applied to smooth reinforcing steel. Construct Build Mater 2012;35:376–84.
[29] NRC. International Critical Tables, vol. 2. Washington (DC): McGraw-Hill, National Research Council (NRC); 1927. p. 116.
[30] ASTM. Standard specification for Portland cement. American Society of Testing Methods (ASTM), C150-07; 2007a.
[31] Stern M, Geary AL. Electrochemical polarization I. A theoretical analysis of the shape of polarization curves. J Electrochem Soc 1957;104(1):56–63.
[32] Aperador W, Mejia de Gutierrez R, Bastidas DM. Steel corrosion behavior in carbonated alkali-activated slag concrete. Corros Sci 2009;51(9):2027–33.
[33] Ghods P, Isgor OB, Bensebaa F, Kingston D. Angle-resolved XPS study of carbon steel passivity and chloride-induced depassivation in simulated concrete pore solution. Corros Sci 2012;58:159–67.
[34] Bruno H, Hostis VL, Miserque F, Idrissi H. Electrochemical behavior of mild steel in concrete: influence of pH and carbonate content of concrete pore solution. Electrochim Acta 2005;51(1):172–80.
[35] ASTM. Standard Test Method for Corrosion Potentials of Uncoated Reinforcing Steel in Concrete. American Society of Testing Methods (ASTM), C876-09; 2009.
[36] ACI 318 Building Code Requirements for Reinforced Concrete, Michigan: American Concrete Institute, 2008.
[37] Mehta PK. Effect of cement composition on corrosion of reinforcing steel in concrete, chloride corrosion of steel in concrete, vol. 629. Philadelphia: ASTM STP; 1977. p. 12–19.
[38] Ford SJ, Shane JD, Mason TO. Assignment of features in impedance spectra of the cement-paste/steel system. Cem Concr Res 1998;28(12):1737–51.
[39] Sagoe-crentsil KK, Glasser FP, Irvine JT. Electrochemical characteristics of reinforced concrete corrosion as determined by impedance spectroscopy. Brit Corros J 1992;27(2):113–8.
[40] Chen W, Du R, Ye C, Zhu Y, Lin C. Study on the corrosion behavior of reinforcing steel in simulated concrete pore solutions using in situ Raman spectroscopy assisted by electrochemical techniques. Electrochim Acta 2010;55(20):5677–82.
[41] May 2012. <http://www.princetonappliedresearch.com/Our-Products/Electrochemical-Software/ZSimpWin.aspx>.
[42] Liu XW, Xiong JP, Lv YW, Zuo Y. Study on corrosion electrochemical behavior of several different coating systems by EIS. Prog Org Coat 2009;64(4):497–503.